Numerical simulation of collapsing vapor bubble clusters close to a rigid wall

[1]Daria Ogloblina*; [1] Steffen J. Schmidt; [1] Nikolaus A. Adams;

[1]*Institute of Aerodynamics and Fluid Mechanics, Technical University of Munich, Germany;*

Abstract

Numerical simulation is a promising way for improvement of physical insight into collapse dynamics for clouds with strong bubble-bubble interaction. The current study adopts the theory proposed by Brennen et al [6] based on "cloud interaction parameter", although the theory is a simplification of realistic cloud collapses, it shows main features, such as shock focusing and enhancement of the resulting shock strength. We offer high quality CFD Simulations of collapsing vapor-bubble clouds close to a rigid wall. The simulations contain physical details such as wave dynamics, bubble deformation and vapor bubble rebound. The simulation time captures several sequential collapses. Our results show different collapse structures as well as different interaction mechanisms of bubbles. We present focusing features as well as unfocused collapses and discuss their effects on material loads. . Increasing the interaction parameter leads to an enhancement of the collapse pressure of individual bubbles, enhanced vapor production during rebound and enhanced load at the wall. An increase in stand-off distance changes the collapse dynamics significantly. Depending on the interaction, rebounds may occur close to the wall, leading to intense secondary collapses.

Keywords: cloud cavitation; cavitation erosion; bubble cluster collapse; bubble interaction parameter;

Introduction

Collapsing single bubbles have been extensively investigated in the past and results obtained by experiments, theory and simulations are broadly represented in the literature [1], [2]. Significantly fewer publications can be found where larger bubble clusters are considered [3-5]. Although there is a simple theory provided by Brennen et al [6], clusters of bubbles are difficult to investigate experimentally. Therefore, numerical simulation of collapsing bubble clusters is a suitable way to enhance physical insight into collapse processes.

To estimate the interaction among bubbles a cloud interaction parameter β was introduced [4]. This parameter is defined as $\alpha_0 \cdot (1- \alpha_0) \cdot A_0^2/R_0^2$, where α_0 is initial cloud void fraction and A_0 and R_0 are the cloud and the bubble radius, respectively. It was shown in previous studies [7], [8] that cloud collapse mechanisms are significantly depending on the cloud interaction parameter. In this investigation the interaction parameter is chosen to be 4, 8 and 11, indicating that bubble interaction is relevant.

In the present work a single-fluid approach coupled with a thermodynamic equilibrium model is adopted. When the grid resolution is sufficiently fine, the thermodynamic equilibrium model implicitly resolves the interface and becomes comparable to a sharp interface technique without surface tension [3]. It enables the prediction of re-evaporation processes, such as bubble rebound.

Two major physical aspects, namely the cloud interaction parameter and the standoff-distance, are investigated. First, a series of three bubble clusters at a fixed stand-off distance from a wall are generated. The radii of the approximately spherical clusters are kept constant while the common radii of the involved bubbles are varied. This leads to three different cloud interaction parameters. In a second series of computations, the cloud interaction parameter is kept constant while four different stand-off distances are investigated.

For all configurations, the dominant collapse mechanism, rebound structures and maximum impact loads are analyzed. A major finding is that the secondary collapse after the first rebound may lead to the highest loads at the solid wall. This indicates that the secondary collapse can considerably contribute to cavitation induced material erosion.

Methodology

The main focus of this investigation is on inertia-driven effects and wave dynamics arising during the collapse of a bubble cloud. Surface tension and viscous effects are neglected and the governing equations are the compressible Euler equations. For this investigation the flow simulation code CaTUM is used [9]. All numerical procedures have been extensively validated and the results have been published in the literature [10-14]. The compressibility of the fluid is taken into account in order to capture shock formation and wave propagation.

Phase change is modelled with equilibrium phase transition, i.e. both phases are in thermal, mechanical and phase equilibrium. In this study, the thermodynamic properties of water (in its liquid and vapor phases) are described by efficient barotropic equations of state. Pure liquid can be modelled by a Tait equation while saturated mixtures are

*Corresponding Author, Daria Ogloblina: daria.ogloblina@tum.de

modelled by a barotropic relation $p = p(\rho)$, which is obtained by integration of the equilibrium speed of sound along an isentrope. The vapor volume fraction of a saturated mixture of liquid and vapor can be derived from the saturation densities of both phases.
As there is insufficient experimental data of "reference clouds" available, a random procedure proposed by *Schmidt et al* [3] is utilized to generate bubble clusters. The following criteria are assumed**:**
1. The bubble cluster covers a spherical domain with a diameter of 30 mm, 150 spherical bubbles of equal radii are randomly generated within it, and the minimum distance between bubbles is one bubble radius. The bubble number density has its maximum at the center of the cloud and follows a *K/r* rule. Here, *K* is a positive constant dependent on the selected bubble radius and *r* is the radial coordinate from the center to the outside of the bubble cluster; **2.**The generated cloud is embedded within a small computational domain of 35x35x40 mm³ which itself is embedded in a larger domain of 4x4x2 m³. In the small domain a fine Cartesian grid is applied in order to minimize numerical errors. The large outer domain contains a hexahedral grid where grid cells are stretched towards the boundary, which are inviscid adiabatic walls; **3.** All bubbles are filled with water vapor while the surrounding domain contains liquid water at an initial pressure of p_∞ = 100 bar. The initial pressure inside the bubbles is equal to the vapor pressure p_{sat} = 2340 Pa at T = 293K. The velocity field is initially at rest. **4.** The effects of surface tension, viscosity, gravity and non-condensable gas content are neglected.

Problem setup

The aim of this investigation is to examine the influence of two parameters (cloud interaction parameter β and stand-off distance d) with respect to the collapse process and on maximum loads at the wall. Therefore, two setups are generated and simulated. For both setups the radius of the generated cloud is A_0 = 15mm and the number of bubbles equals 150 for all cases. Setup details are shown in the **Table 1.**
The first setup contains three random clouds with different initial bubble radii of R_0 = 0.5 mm, 1.0 mm and 1.5 mm, and the interaction parameter β equals to β = 4, 8 and 11 respectively. The positions of individual bubbles within this setup are case dependent. The stand-off distance d = 3.2 mm of the cloud from the wall is kept constant.
The second setup is designed to investigate the effects of different stand-off distances to the wall. The clouds are identical in terms of bubble distribution and initial bubble radius, which is R_0 = 1 mm. The stand-off distance is defined as the minimum distance between the virtual surface of the cloud and the bottom wall and equals to d = 1.2 mm, 3.2 mm, 6.0 mm and 10.0 mm.

Parameters	Setup I	Setup II
Bubble radius, R_0 [mm]	R_0 = 0.5, 1.0, 1.5	R_0 = 1.0
Vapor ratio, α_0 **%** [-]	α_0 = 0.4%, 3%, 8%	α_0 = 3%
Cloud interaction parameter, β [-]	β = 4, 8, 11	β = 8
Standoff distance, d [mm]	d = 3.2	d = 1.2, 3.2, 6.0, 10.0

Table 1: Properties of the designed setups.

Results

Setup I: Variation of interaction parameter β. The variation of this quantity will affect the cloud collapse behaviour, e.g. the strength of bubble-bubble interaction, intensities of collapses of individual bubbles and of the focused collapse at the center of the bubble cluster.
Figure 1 shows the dimensionless temporal evolution of the equivalent radius R_{equiv} as well as of the output from the numerical pressure transducer at the wall for all three interaction parameters. It can be seen that the relative duration of the cloud collapse is about 60% of the case-specific Rayleigh time [15] for all three configurations. However, the subsequent re-evaporation is quite different between the three cases. The smaller the interaction parameter, the more pronounced is the delay between collapse and rebound. This tendency seems to hold for subsequent collapses of re-evaporated structures as well.
With respect to the evolution of the pressure recorded at the wall, the following trends are found. Weak interaction leads to a low frequency increase of the pressure. Higher interaction causes high frequency pressure oscillations and larger amplitudes (see **Fig. 1**). However, a comparison of the maximum pressure recorded by the numerical transducers subsequent to the collapse phases show an unexpected behaviour, as depicted in **Figure 2**. While the load at the wall

*Corresponding Author, Daria Ogloblina: daria.ogloblina@tum.de

decays more or less monotonically in case of strong interaction, it stays approximately constant in case of very weak interaction. In case of intermediate interaction (here for β = 8) a nonlinear trend is predicted. In this case, the most intense load at the wall occurs after the secondary collapse.

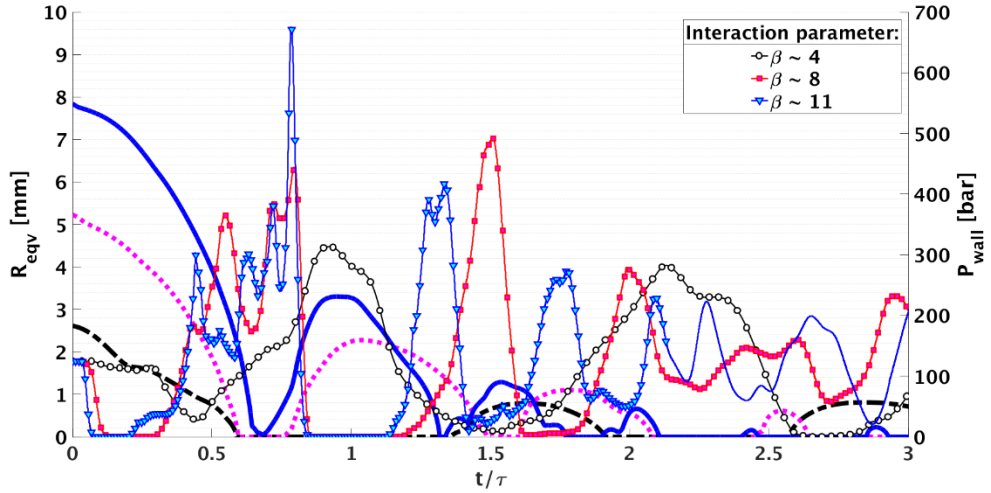

Fig. 1: Setup I: Thick line – equivalent bubble radius evolution; thin line - pressure recorded by the wall transducer; both against dimensionless time scaled with Rayleigh time for equivalent bubble

Setup II: Variation of stand-off distance d. Figure 3 shows the dimensionless temporal evolution of the equivalent radius R_{equiv} as well as of the output from the pressure transducer at the wall for all four stand-off distances. Again, the duration of the collapse of the primary cloud is approximately 60% of the Rayleigh time of an equivalent bubble for all cases. It can be seen that the duration of the primary collapse is slightly shorter when the stand-off distance is increased. The wall partially confines the flow field for small stand-off distances, while it has minor effects when the cloud is located sufficiently far away from it. As β = 8, moderate interaction intensity and collapse focussing occurs for all cases.

An unexpected behaviour is seen for the second and the third rebound of vapour structures. The maximum amount of vapour is inversely proportional to the initial stand-off distance during the first rebound. This is, however, not the case for the second rebound, where the tendency seems to be reversed. The output of the numerical pressure transducer at the wall shows that the pressure increases during the end of a collapse phase and features several maxima during collapse and rebound (**Fig. 3**). This observation holds for all four stand-off distances and all computed collapse-rebound-cycles.

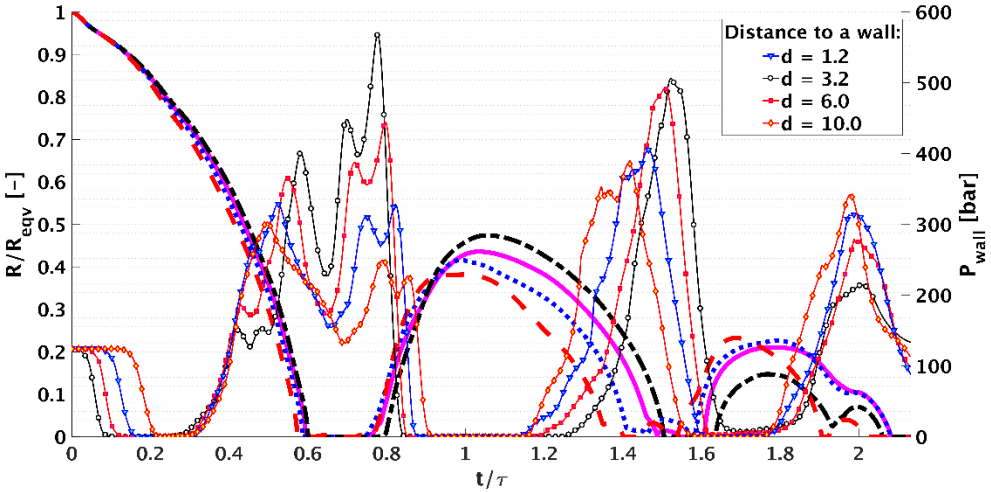

Fig. 3: Setup II: Thick line – equivalent bubble radius evolution; thin line - pressure recorded by the wall transducer; both against dimensionless time scaled with Rayleigh time for equivalent bubble

*Corresponding Author, Daria Ogloblina: daria.ogloblina@tum.de

Figure 4 shows maximum pressures recorded at the wall after three collapse phases for all investigated stand-off distances. As expected, the intensity of the primary collapse is inversely proportional to the initial stand-off distance. This trend can be explained by the location of the focal point of the collapse, which locates more closely to the wall if the stand-off distance is smaller. Interestingly, the pressures recorded after the secondary collapses and especially subsequent to the third collapses show a nonlinear behaviour: for a stand-off distance of d = 1.2 mm a decrease in pressure is predicted for subsequent collapses. In case of d = 3.2 mm to d = 10 mm the pressures recorded after the secondary collapses exceed those recorded after the primary collapses. Although the collapse intensities decrease when comparing collapses 2 and 3, an unexpected trend is found: the pressures recorded after the third collapse are now proportional to the initial stand-off distance.

In order to understand this behavior, the maximum vapor volume during rebound and the position of the focal point of the subsequent collapse are investigated. The maximum vapour volume (or the radius of the equivalent bubble) is reversed in order when comparing rebound 1 to rebound 2. Additionally, the focal points are shifted towards the wall in all cases. Both contributions affect the pressure recorded at the wall. However, the maximum pressure at the focal point of a (focussed) cloud collapse is not necessarily related to the pressure recorded at the wall. For example, in case of d = 10 mm, the pressure detected at the focal point is much higher during the primary collapse compared to the subsequent collapses.

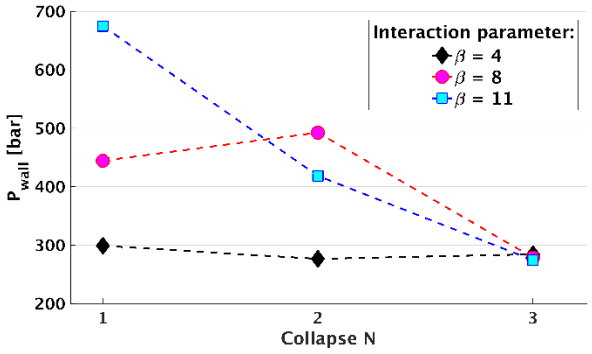

Fig. 2: Maximum pressure peaks recorded by the numerical wall pressure transducer subsequent to consecutive collapses

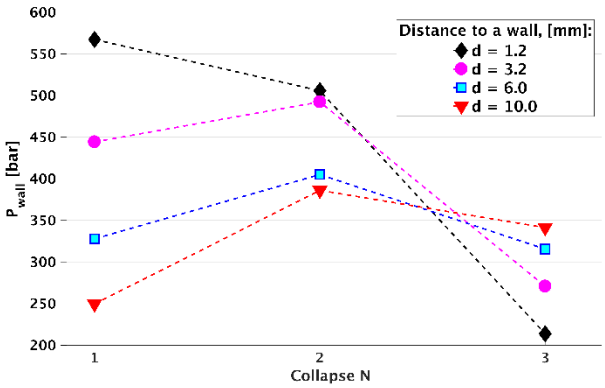

Fig. 4: Pressure peaks caused by primary collapse and two rebounds. Pressure of primary collapse is proportional to cloud distance to the wall. Intensity of second rebound collapse reverses intensity of primary collapse

Conclusion

This study shows the effects of the cloud interaction parameter and of the stand-off distance on the collapse of a cloud of vapor bubbles in a liquid ambient. Maximum loads at the surface are recorded by application of a numerical force/pressure transducer. Two series of numerical simulations with in total seven cases were performed and analyzed. The major findings are:

1. The cloud interaction parameter proposed by Brennen [4] is a suitable measure for bubble interactions and shock focusing. From this investigation it can be concluded that an interaction parameter of O(1) or smaller results in weak interaction without shock/collapse focusing. Once the interaction parameter is O(10) or higher, strong interaction and pronounced focusing are to be expected. Increasing the interaction parameter β leads to an enhancement of geometrical focusing and of the collapse pressure of individual bubbles. Additionally, the intensification of vapor production close to the wall during rebound is observed and, consequently, an increase of maximum loads at the wall is detected.

2. The stand-off distance is well suited to quantify the intensity of the primary cloud collapse with respect to its erosive potential at an adjacent material surface. However, this investigation shows that secondary and even third collapses subsequent to rebound processes can cause intense loads at material surfaces, too. Therefore, primary collapses and collapses of rebounded vapor structures are both potentially relevant for erosion. The primary collapse induces a velocity field which targets towards the wall and rebounding vapor patters are advected with this velocity field. Secondary and tertiary collapses occur closer and closer to the wall and the resulting load at the wall increases as well. Further studies of this work will include non-homogeneous initial bubble radii in order to assess effects of micro-scale details aside from macro-scale quantities such as the interaction parameter. Further numerical developments will be the inclusions of viscous effects and non-condensable gas content.

*Corresponding Author, Daria Ogloblina: daria.ogloblina@tum.de

a = 0.4%, β = 4 ***a = 3%, β = 8*** ***a = 8%, β = 11***

a – c: Pressure field and vapor iso-surface after the prior collapse before the second. In the first case no pronounced cloud appears during rebound. In the other two cases vapor rebound occurs right at the wall, a secondary cloud in the center of the domain. Clouds collapse from top to bottom in both latter cases.

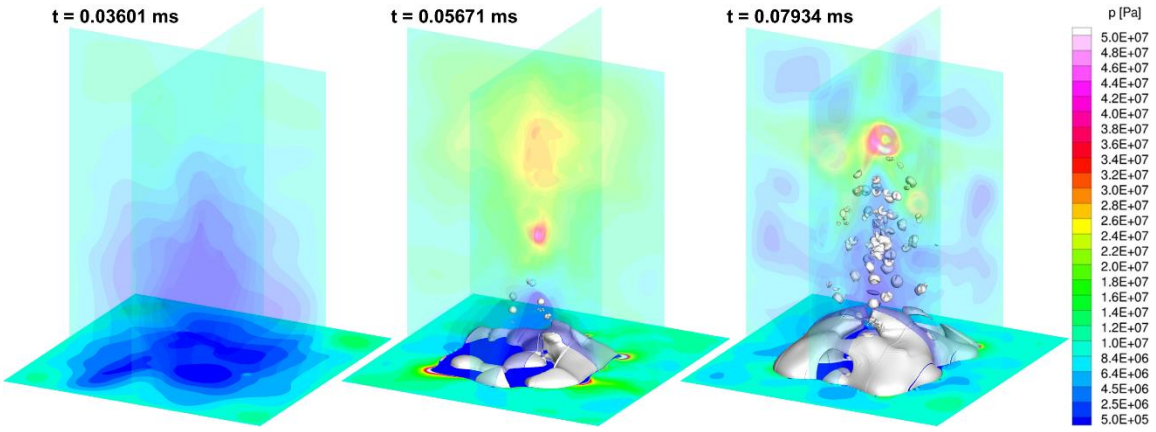

d – f: Pressure field and vapor iso-surface at the second collapse. In the first case relatively small collapse of $1.1 \cdot 10^4$ bar appears above the wall. In the middle case vapor at the wall collapses producing pressure peak of $1.78 \cdot 10^4$ bar. The last case shows the most violent collapse at the wall of $2.26 \cdot 10^4$ bar. This type of collapse is supposed to be highly relevant for cavitation erosion.

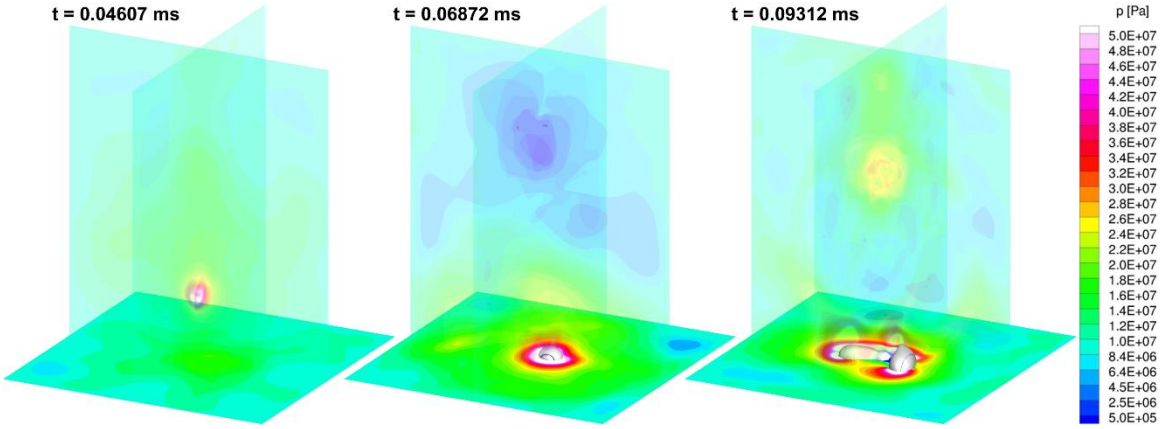

g – i: Pressure field and vapor iso-surface at the third collapse. In the first case the position of a collapse shifts further towards the wall and it occurs right at the wall with pressure magnitude $0.4 \cdot 10^4$ bar. In the middle case the third collapse of $0.8 \cdot 10^4$ bar is also at the wall. In opposite, the last case shows no significant impact on the wall since vapor structures are driven far above the wall and then collapse with $0.07 \cdot 10^4 \cdot$bar. Two latter clouds collapse from bottom to top.

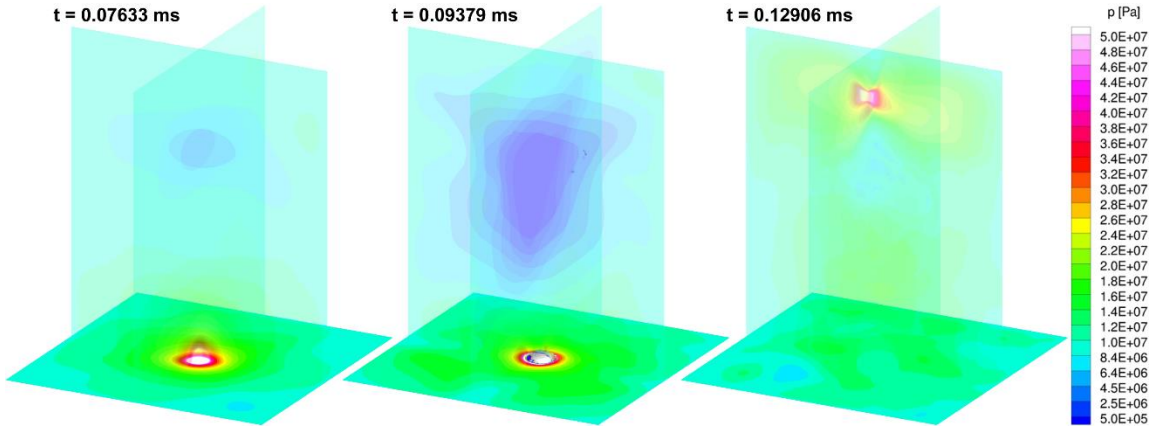

Fig. 5. Setup I: Pressure field depicted on two intersecting slices of the inner domain. White structures are iso-surfaces of vapor ratio equal to 5%. The initial vapor parameter and therefore interaction parameter increase from left to right.

*Corresponding Author, Daria Ogloblina: daria.ogloblina@tum.de

Acknowledgment

This study is part of a project that has received funding from the European Union's Horizon 2020 research and innovation programme under grant agreement № 642536.

References

[1] Lauer, E. Hu, X. Y. Hickel, S. Adams, N. A. (2012). *"Numerical modelling and investigation of symmetric and asymmetric cavitation bubble dynamics"*. Comput. Fluids 69, 1–19.
[2] Fujikawa S. and Akamatsu T.(1980).*"Effect of the non-equilibrium condensation of vapour on the pressure wave produced by the collapse of a bubble in a liquid."* J. Fluid Mech. 97, 481–512.
[3] Schmidt, S.J., Mihatsch, M., Thalhamer, M., Adams, N.A. (2011). *"Assessment of the Prediction Capability of a Thermodynamic Cavitation Model for the Collapse Characteristics of a Vapor-Bubble Cloud."* WIMRC Cavitation Forum..
[4] Wang, Y.-C., Brennen, C. E. (1999). "*Numerical Computation of Shock Waves in a Spherical Cloud of Cavitation Bubbles,"* J. Fluids Eng 121(4).
[5] Rossinelli, D., Hejazialhosseini, B., Hadjidoukas, P., Bekas, C., Curioni, A., Bertsch, A., Futral, S., Schmidt, S. J., Adams, N. A., Koumoutsakos, P. (2013). *"11 PFLOP/s simulations of cloud cavitation collapse"* International Conference on High Performance Computing, Networking, Storage and Analysis.
[6] Brennen C. E. (1995) "*Cavitation and Bubble Dynamics"*, Cambridge University Press.
[7] d'Agostino, L., Brennen, C. E., (1983).*"On the acoustical dynamics of bubble clouds".* AESME Cavitation and Multiphase Flow Forum, 72-75.
[8] d'Agostino, L., Brennen, C. E. (1999). *"Acoustical absorption and scattering cross sections of spherical bubble clouds,"*J. Acous. Soc. Am. 84, 2126-2134.
[9] Sezal I. H. (2009). "*Compressible Dynamics of Cavitating 3-D Multi-Phase Flows"*, PhD Thesis, TUM.
[10] Egerer, C. P., Schmidt, S. J., Hickel, S., Adams, N. A. (2016). *"Efficient implicit LES method for the simulation of turbulent cavitating flows."* J. Comp Phys.
[11] Mihatsch, M., Schmidt, S.J., Thalhamer, M., Adams, N.A. (2012). *„Quantitative Prediction of Erosion Aggressiveness through Numerical Simulation of 3D Unsteady Cavitating Flows."* CAV2012.
[12] Budich, B., Schmidt, S. J., Adams, N. A. (2016). *"Numerical Investigation of Condensation Shocks in Cavitating Flow."* 31st Symposium on Naval Hydrodynamics.
[13] Budich, B., Schmidt, S. J., Adams, N. A. (2016) *"Implicit Large Eddy Simulation of the Cavitating Model Propeller VP1304 using a Compressible Homogeneous Mixture Mode."* 31st Symposium on Naval Hydrodynamics.
[14] Beban B., Legat S., Schmidt S.J., Adams N. A. (2015). "*On instationary mechanisms in cavitating micro throttles."* CAV2015, J. Phys 656.
[15] Franc, J.-P., Michel, J.-M. (2004). "*Fundamentals of Cavitation."* Kluwer Academic Publishers.

*Corresponding Author, Daria Ogloblina: daria.ogloblina@tum.de